SCALE-BY-SCALE ENERGY AND TEMPERATURE VARIANCE BUDGETS IN A TURBULENT MIXING LAYER

L. Djenidi*, R.A. Antonia and S. Rajagopalan
School of Engineering
The University of Newcastle
NSW 2308, Australia
* lyazid.djenidi@newcastle.edu.au

ABSTRACT

Velocity and temperature measurements are carried out in a mixing layer of a heated turbulent round jet with the aim of investigating how the large scale vortical structures that characterize the mixing layer affect both the energy and scalar variance transport terms. The assessment is performed through the measurements of the second and third-order velocity and temperature structure functions.

Compared with the jet centreline, the structure functions for both velocity and temperature are altered in the mixing layer. The modification is consistent with the presence of large scale coherent structures in the mixing layer. For example, the approach to the limiting value of 2 for the second-order structure functions, which is monotonic on the jet centreline, undergoes an oscillation in the mixing layer. An oscillation is also observed for the third-order structure functions in the mixing layer. The scale-by-scale energy budgets suggest that the non-homogeneity in the mixing layer contributes more to the budget than on the jet centreline.

PAPER TITLE AND AUTHOR(S)

Transport equations for second-order (longitudinal) velocity $(\delta u)^2$ (= $(u(x+r) - u(x))^2$), and temperature $(\delta\theta)^2$ (= $(\theta(x+r) - \theta(x))^2$) structure functions were written for homogeneous isotropic turbulence by Danaila et al. (1999) and tested using measurements in slightly heated grid turbulence. These equations, shown below

$$< (\delta u)^3 > -6\nu \frac{d}{dr} < (\delta u)^2 > -\frac{3}{r^4}\int_0^r s^4 \frac{\partial}{\partial t} < (\delta u)^2 > ds = -\frac{4}{5} < \varepsilon > r \quad (1)$$

$$< \delta u (\delta\theta)^2 > -2k \frac{d}{dr} < (\delta\theta)^2 > +\frac{1}{r^2}\int_0^r s^2 \frac{\partial}{\partial t} < (\delta\theta)^2 > ds = -\frac{4}{3} < \varepsilon_\theta > r \quad (2)$$

($< \varepsilon >$ and $< \varepsilon_\theta >$ are the mean turbulent kinetic energy dissipation rate and mean temperature dissipation rate respectively, ν is the kinematics viscosity, k the molecular diffusivity, r is the longitudinal increment; the angular brackets denote time averaging), correspond to the equations for two-point velocity and temperature correlation functions first written by Karman and Howarth (1938) and Corrsin (1951) respectively and effectively represent scale-by-scale budgets of the turbulent energy and temperature variance at a location in the flow. At a sufficiently large Reynolds number, these equations reduce to the equations of Kolmogorov (1941) and Yaglom (1949) (i.e. the third term on the left hansd side of each equation is zero). However, unlike the latter equations, they can describe the effect of the non-stationarity in homogeneous isotropic turbulence (through the intregral terms of Eqs. (1) and (2)) at finite Reynolds numbers and hence predict the approach to the asymptotic "4/5" and "4/3" laws as the Reynolds number increases (e.g. Antonia and Burattini, 2006). Indeed, at large r, the integral term becomes the major contributor, while the first and second terms on the left hand sides become negligible.

Modified forms of these equations have been written for more complicated flows (e.g. Danaila et al., 2001 for a turbulent channel flow and Burattini et al., 2005 for a self-preserving turbulent round jet) to account for the effects that different types of non-stationarity or non-homogenity can have on the magnitude of the energy transfer term represented by the third-order velocity structure function. Danaila et al. (2004) showed that equation (1) is closely satisfied by data in grid turbulence and a turbulent round jet (along the axis). Burattini et al. (2005) provided further confirmation for a turbulent round jet. They also pointed out that equation (1) may not be approriate in the region away from the centerline, and that extra terms accounting for the production and decay of the turbulent energy should be added to the equation.

The objective of the present work is to extend the above approach to a slightly heated mixing layer in order to identify the effect that the large scale vortical structures which characterize this flow has on both on the energy and scalar variance transport terms. Experimental results are given for both second and third-order velocity structure functions as well as second-order temeperature structure functions and third-order mixed velocity-temperature structure functions in the mixing layer of a turbulent round jet. They are compared with corresponding results on the jet centerline at a distance of 20 nozzle diameters from the nozzle exit plane. We also present preliminary scale-by-scale velocity and temperature variance budgets.

EXPERIMENTAL SETUP

Mesurements are made in a low speed axisymmetric jet with a of a circular nozzle of diameter D = 55*mm*. Air is supplied by a variable speed centrigugal blower to a diffucer, settling chamber followed by a 9:1 contraction (Figure 1). A mixing layer develops downstream of the exit section. At the jet exit, the velocity U_j is 5*m/s* while the temperature *Tj* (relative to ambient) is 13.7 deg C. Heat, treated here as a passive scalar, was introduced via an electric fan heater placed at the inlet of the blower. The jet exit tempertaure could be varied by changing the heater current. The boundary layer at the nozzle has not been tripped for this study. A pair of parallel single wires have been used – with the hot wire (wollaston diameter = 2.5μm) operated in constant temperature mode and the cold wire (wollaston diameter = 0.63μm) by a constant current (100μA) circuit. The separation between the hot and cold wires was approximately 0.75 mm. Mean and rms velocity and temperature distributions between x/D=2 and x/D = 5 have confirmed that the flow is self-preserving, with an effective origin at x = 0. Longitudinal (x-direction) movement of the probe was achieved with a motorised traversing unit while the lateral (y-direction) movement was achieved by using a height gauge with a resolution of 0.01 mm. Velocity and temperature fluctuation signals were filtered at 5 kHz and sampled at 10 kHz using a 12 bit data logger.

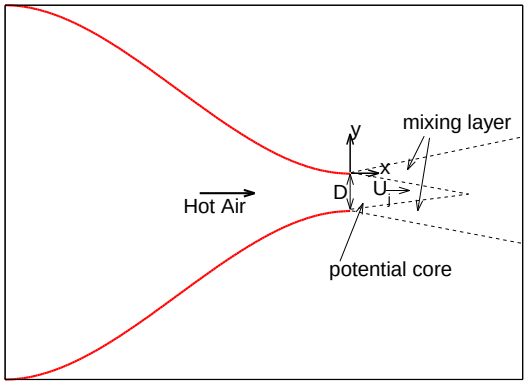

Figure 1. Stetch of the jet and the coordinate system.

RESULTS

Mean and fluctuation components

Figure 2 shows the mean velocity and temperature profiles across the mixing layer at x/D = 4 and 20. The origin y = 0 corresponds to the radial location of the nozzle lip and y = -25mm is the jet centreline (see Figure 1).

The mean velocity and temperature at x/D = 4 are maximum at the centreline and decrease with increasing y, as expected in a jet flow. For x/D = 20, both the velocity and temperature profiles are almost flat, reflecting the spreading of the jet wake. However, although not clearly visible in the figure due the plotting scale, both profiles have their maximum shifted at around y = 12*mm* for the velocity and y = 0 for the temperature. The main feature of Figure 2 is the change in the rate of decrease of the mean temperature profile around y = 0. This change is reflected in the rms temperature profile (Figure 3) which exhibits a minimum at the same y position.

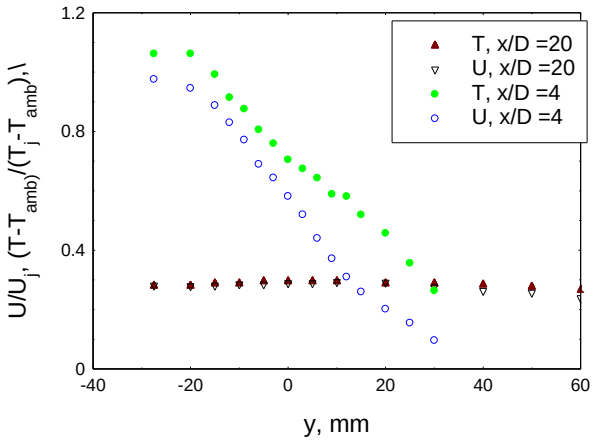

Figure 2. Mean velocity and temperature profiles across the mixing.

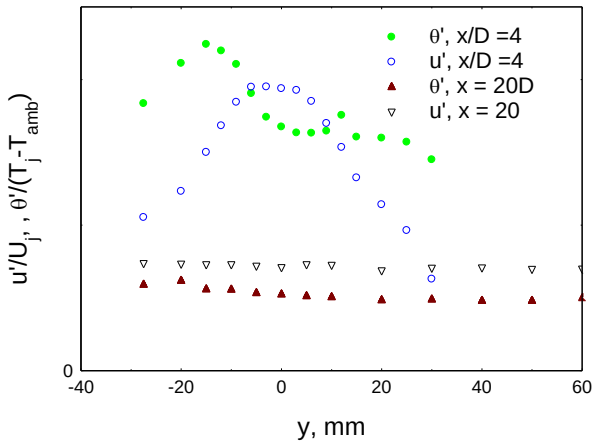

Figure 3. Profiles of u' and θ' across the mximg layer and at x/D=20[

Interestingly, a local minimum in θ' occurs almost at the location where the velocity rms, u', is maximum. At x/D = 20, both the rms velocity and temperature distributions are almost flat.

Dissipation parameters

Figure 4 shows radial distributions of the normalized dissipation parameters $C_\varepsilon = \langle\varepsilon\rangle L_u/u'^3$ and $C_\theta = \langle\varepsilon_\theta\rangle L_u/(u'\theta'^2)$ at x/D = 4 (L_u is the integral length scale inferred from the autocorrelation of u by assuming that U_j is the appropriate convection velocity; angular brackets denote time averaging). The isotropic values of $\langle\varepsilon\rangle$

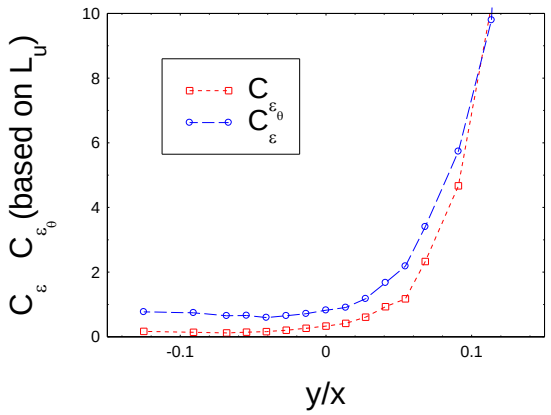

Figure 4. Radial distributions of C_ε and C_{ε_θ} in the mixing layer (x/D = 4)

$$< \varepsilon >_{iso} = 15\nu < (\partial u / \partial x)^2 > \quad (3)$$

and $< \varepsilon_\theta >$

$$< \varepsilon_\theta >_{iso} = 3\kappa < (\partial \theta / \partial x)^2 > \quad (4)$$

have been used for these estimates. The magnitude of both parameters is approximately constant over the high speed side (y < 0) of the layer, although C_ε is consistently larger than C_{ε_θ} . This difference would be increased further if L_u were replaced by L_θ in the definition of C_{ε_θ} .

Second and third-order structure functions

The second and third order structure functions are shown in Figures 5 and 6, where the normalization is by u' and θ' since $< \varepsilon >_{iso}$ and $< \varepsilon_\theta >_{iso}$ are unlikely to be sufficiently accurate approximations for $< \varepsilon >$ and $< \varepsilon_\theta >$ for x/D = 4. The second-order moments of the increments $\delta u = <u(x+r) - u(x)>$ and $\delta\theta = <\theta(x+r) - \theta(x)>$ (Fig. 4) differ significantly between the high speed side of the mixing layer and the axis of the jet (x/D=20). In particular, $< (\delta u)^2 >$ and $< (\delta\theta)^2 >$ approach 2, the expected limit when r is sufficiently larger than L_u, differently. In the mixing layer, both $< (\delta u)^2 >$ and $< (\delta\theta)^2 >$ have a maximum near $r/L_u \approx 2.5$ prior to reaching 2. In the self-preserving jet, 2 is approached in a monotonic manner. For the third-order moments $< (\delta u)^3 >$ and $< (\delta u)(\delta\theta)^2 >$ (Fig 5.), the difference between the mixing layer and the self-preserving jet is more emphatic. In the former case, the distribution is quasi-periodic with a strong change of sign, reflecting the presence of the relatively large scale coherent structures whereas there is no change of sign at x/D =20.

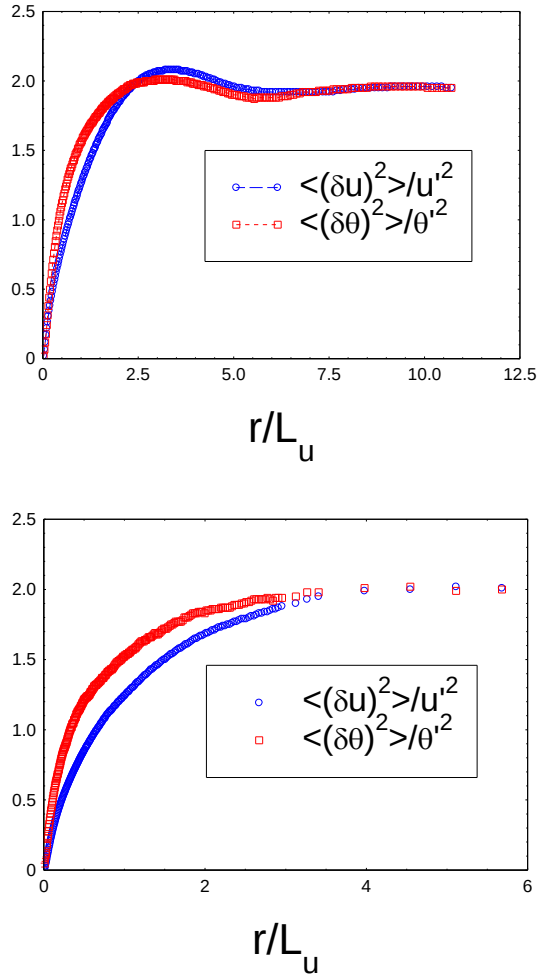

Figure 5. Second-order structure functions. Top: mixing layer (x/D = 4, y/x = -0.027), bottom: jet axis(x/D = 20).

While the non-monotonic approach to 2 has been observed (Antonia et al. 2002) for $< (\delta v)^2 >$ (v is the lateral velocity fluctuation) in a turbulent wake (at a distance of 70d downstream of a circular cylinder of diameter d), there is no indication of a change of sign for $< (\delta u)^3 >$, implying a much stronger inhomogeneity for the mixing layer.

Velocity and temperature variance scale by scale budgets

It has already been stated that equations (1) and (2) are not valid for the mixing layer. Extra terms are likely to be required to account for the production and diffusion terms which are absent in a grid turbulence. Nonetheless one can write these equations in the following simplified manner

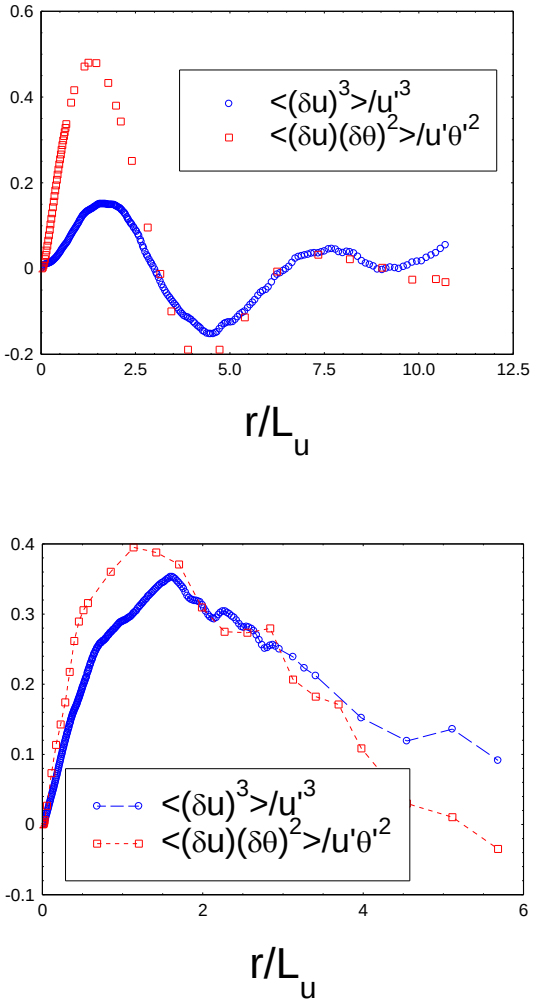

Figure 6: Third-order structure functions. Top: mixing layer (x/D = 4, y/D= -0.027), bottom: jet axis (x/D = 20)

$$< (\delta u)^3 > -6\nu \frac{d}{dr} < (\delta u)^2 > + I_u = -\frac{4}{5} < \varepsilon > r \qquad (5)$$

$$< \delta u (\delta\theta)^2 > -2k \frac{d}{dr} < (\delta\theta)^2 > + I_\theta = -\frac{4}{3} < \varepsilon_\theta > r \qquad (6)$$

where I_u and I_θ include contributions from production, diffusion and non-stationarity of the second-order moments. I_u and I_θ can be deduced from equations (5) and (6) if the first and second terms on the left hand side as well as the terms on the right hand side of these equations are available. The reliable determination of the latter terms, which contain the dissipation rates, represents a major experimental challenge since several velocity and temperature fluctuation derivatives are required in order to obtain $<\varepsilon>$ and $<\varepsilon_\theta>$ accurately. Crude estimates for these quantities are provided using local isotropy , viz. eqs. (3) and (4). It is also worth emphasizing that the quality of the data and data processing are important. For example, one can recall the errors caused by the finite spatial resolution of the probe, and the need to apply a spectral correction before the "correct" values of $< \varepsilon >_{iso}$ and $< \varepsilon_\theta >_{iso}$ can be obtained. In the present work we use a relatively

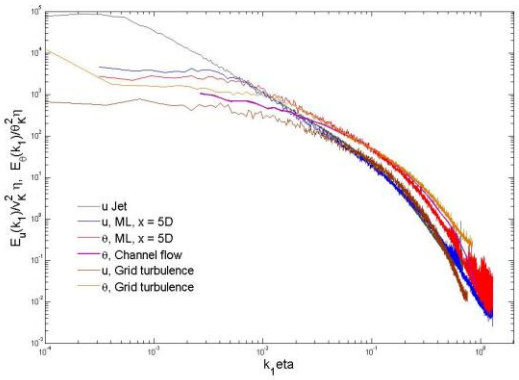

Figure 7: Velocity and temperature spectra in the mixing layer, x/D = 5, y/D= 0.

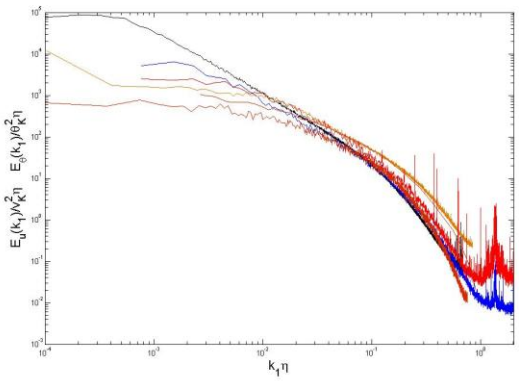

Figure 8: Velocity and temperature spectra in the jet axis, x/D = 20. (Same symbols as in Fig 7)

simple way to bypass these difficulties. The measured spectra normalised by Kolmogorov scales are compared with reference spectra which are known to be relatively accurate in both the dissipative range and the upper end of the inertial range. Local isotropy was first used to normalise the spectra before the matching process is carried out. The reference spectra are those measured in slightly heated grid turbulence (Antonia et al., 2004), where the actual values of $< \varepsilon >$ and $< \varepsilon_\theta >$ were inferred from

$$< \varepsilon > = -\frac{U_0}{2} \frac{d < q^2 >}{dx} \qquad (7)$$

$$< \varepsilon_\theta >= -\frac{U_0}{2}\frac{d < \theta^2 >}{dx} \qquad (8)$$

and are therefore know with reaonably good accuracy.

Using a trial and error procedure, the present values of $< \varepsilon >$ and $< \varepsilon_\theta >$ are adjusted until the measured spectra agree as closely as possible with the reference spectra in part of the dissipative range as well as the upper end of the scaling range. Figures 7 and 8 illustrate the approach and show the "adjusted" velocity and temperature spectra at x/D = 4 and 20. As well as the grid turbulence spectra, we show spectra obtained in a large Reynolds number plane jet (Pearson and Antonia, 2001) and a slightly heated fully developed turbulent channel flow (Antonia and Abe 2009). One can notice the relatively good collapse between the grid turbulence data and both the jet and DNS channel flow data, suggesting that the spectra present a quasi-universal behaviour in the higher end of the inertial range and over part of the dissipative range, at least for the Reynolds numbers used in these studies. This provides some confidence in our methodololgy for estimating the dissipation rates.

While for x/D = 5 (Figure 7) the value of $<\varepsilon_\theta >_{adjusted}$, the adjusted temperature variance dissipation rate, is about 1.35 $<\varepsilon_\theta >_{iso}$, that of $< \varepsilon >_{adjusted}$ is found to be equal to $< \varepsilon >_{iso}$ (i.e. no adjustement was required). For x/D = 20 (Figure 8) we obtained $<\varepsilon >_{adjusted}$ = 0.50 $<\varepsilon >_{iso}$ and $<\varepsilon_\theta >_{adjusted}$ = 0.20 $<\varepsilon_\theta >_{iso}$. It is clear that the measurements at this x/D location, where values of both velocities and temperature are quite low, suffer from noise contamination which affects both the velocity and temperature gradients. This leads to poor estimates of $< \varepsilon >_{iso}$ and $< \varepsilon_\theta >_{iso}$. through expressions (3) and (4).

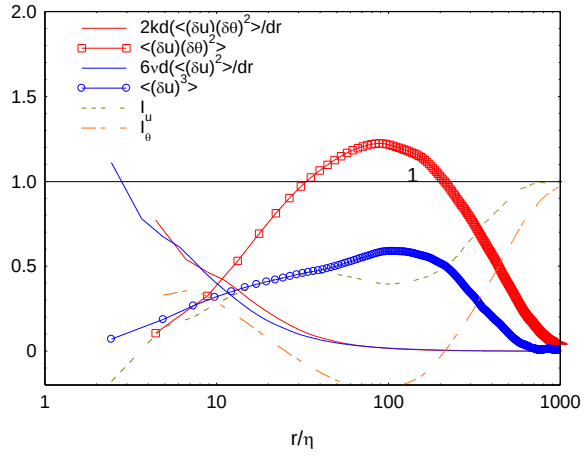

Figure 9: Terms in equation (5) and 6) for x/D = 4, in the mixing layer (y/D = 0)

The adjusted values are used for displaying the terms of the scale-by-scale budgets. All terms of equations (5) and (6) are displayed in Figure 9 for x/D = 5 and Figure 10 for x/D = 20. Terms I_u and I_θ are calculated from the equations using the measured values of the remaining terms. The terms of equation (5) and (6) have been normalized by $4/5<\varepsilon>r$ and $4/3<\varepsilon_\theta >r$, respectively. As expected, the viscous term of equ. (5) dominates the budget for small separations and drops to zero as the separation becomes large. While its temperature counterpart term appears to be behave as expected, i.e. becoming dominant as r/η decreases, that for x/D = 20 reflects the spectral attenuation (see Figure 8). The third-order term for both the velocity and temperature reaches a maximum at r/η of about 100 and 40 for x/D = 5 and 20, respectively. Providing support for the validity of our methodology for estimating the dissipation rates, is the fact that the present velocity scale-by-scale budget on the jet axis is similar to that of $<\delta q^2>$ ($\delta q^2 = \sum_i \delta u_i^2$, i = 1, 2, 3) shown by Burattini et al. (2005). Interestingly, these authors showed that the major contributor to I_q stems from the decay of large scale energy. They also showed that the production is not negligible.

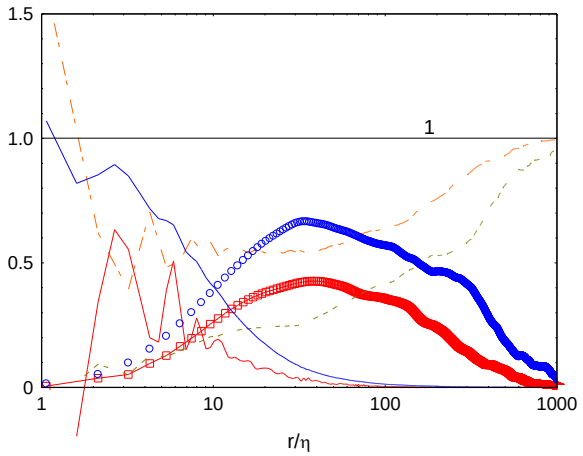

Figure 10: Terms in equs. (5) and (6) on the jet axis at x/D = 20. Same symbols as in Fig 9.

Comparing the velocity budget in the mixing layer with that on the jet axis (Figure 11) one can notice some interesting features. Firstly, the viscous terms ($6\nu d(<(\delta u)^2>)/dr$) collapse remarkably well into a single curve. This certainly reinforces the universal behaviour of this term at small separations. Secondly, the third order term ($<(\delta u)^3>$) in the mixing layer deviates from that in the jet axis in the region $10 < r/\eta < 100$, where it is smaller. Such deviation, within this separation range, would reflect structural differences between the mixing layer and the jet flow, at least on the jet axis. This is consistent with the idea that the production term should be stronger in the mixing layer than on the jet centreline. This would not be surprising considering that the mean velocity gradient and the Reynolds shear stresses are larger in the mixing layer than on the jet axis which should results in a stronger production of energy. Finally, structural differences between the mixing layer and the jet flow on the axis should also be reflected in the various components contributing to I_u. This term exhibits a hump at about r/η = 40 in the mixing layer (Figure 7), whilst it increases monotonically on the jet axis (Figure 8). At this stage, it is not clear whether the behaviour of I_u in the mixing

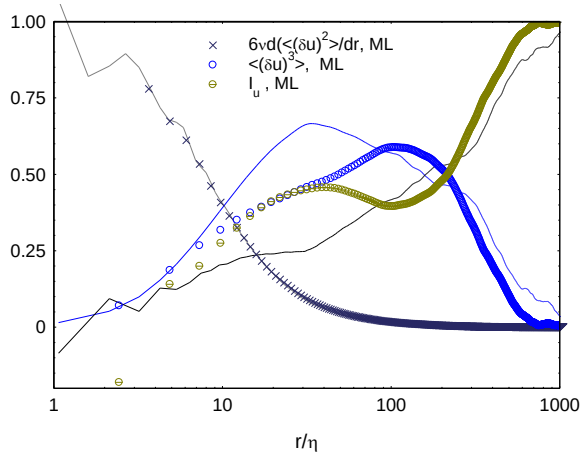

Figure 11: Terms of equs. (5) in the mixing layer (symbols) and the jet axis (lines) .

layer is genuine or not. Clearly, more measurements not only at the same *x/D* and *y/D* locations as in this study but also across the mixing layer are required to adequately shed light onto the behaviour of the velocity scale by scale budget in the mixing layer and off-axis region.

While the measured velocity scale-by-scale budgets seem plausible, those of the temperature variance, at least for the mixing layer, display an anomalous behaviour, as reflected by the maximum value of $3<(\delta u)(\delta\theta)^2>/(4<\varepsilon_\theta>r)$, which exceeds the value of one. This overshoot, while unexpected, may not be impossible nor incorrect. This issue is currently being investigated.

CONCLUSIONS

Velocity and temperature measurements are carried out in a mixing layer developing in a heated axisymmetric jet with the view to assess how the coherent structures in the mixing layer affect the scale-by-scale budgets of the velocity and temperature variances. The results are compared with those obtained on the axis of the self preserving jet. It is observed that the second and third-order structure functions in the mixing layer reflect the presence of strong coherent structures. For example, both the second and third-order structure functions show oscillations at relatively large scales which are absent on the axis of the jet. This clearly highlights the non-homogeneity of the mixing layer. Further, the data seem to indicate that this non-homogeneity has a stronger contribution to the scale-by-scale energy budget in the mixing layer than on the jet centreline. Interestingly, this confirms Burattini et al.'s (2005) argument that extra terms, reflecting inhomogeneities in the region away from the jet centreline, need to be formulated and added to their scale-by-scale energy budget equation (eq. 29 in their paper). It is therefore of interest to further investigate both the mixing layer and the region away from the jet centreline to appraise the contributions from terms in the velocity and temperature variance transport equations which are associated with the inhomogeneity.

REFERENCES

Antonia R A and Abe H 2009, Scaling range behaviour of velocity and passive scalar spectra in a turbulent channel flow, *in Proc. of 6th Int. Symp. on Turbulence, Heat and Mass Transfer* (*Hanjalic Nagano and Jakarlic, eds*.) Rome, Italy, Sept. 14-18.

Antonia R A and Burattini P. 2006 Approach to the 4/5 law in homogeneous isotropic turbulence, *J.Fluid Mech.*, **550**, 175-184.

Antonia R A and Mi J 1993 Temperature dissipation in a turbulent round jet *J. Fluid Mech.* **250**, 531-551.

Antonia R A, Smaley R J, Zhou T, Anselmet, F and Danaila L, 2004, Similarity solution of temperature structure functions in decaying homogeneous isotropic turbulence, *Phys. Rev. E* **69**, 016305

Antonia R A Zhou T and Romano G P 2002 Small-scale characteristic of two-dimensional bluff body wakes, *J. Fluid Mech.***459**, 67-92.

Burattini P, Antonia RA and Danaila L 2005 Scale-by-scale energy budget on the axis of a turbulent round jet, *J. Turbulence*, **6**, DOI: 10.1080/14685240500213744.

Corrsin S 1951 The decay of isotropic temperature fluctuations in an isotropic turbulence, *J. Aero. Sci.*, **18**, 417-423.

Danaila L, Anselmet F, Zhou T and Antonia R A 1999, A generalization of Yaglom's equation which accounts for the large-scale forcing in heated decaying turbulene, *J. Fluid Mech.*, **391**, 359-ics, 6, 128372.

Danaila L, Anselmet F, Zhou T and Antonia R A 2001, Turbulent energy scale budget equation in a fully developed channel flow, *J. Fluid Mech.*, **430**, 87-109.

Danaila L, Antonia R A and Burattini P, 2004, Progress in studying small-scale turbulence using "exact" two-point equations, *New Journal of Phys.*, **6**, 1-23.

von Karman T and Howarth L 1938 On the statistical theory of isotropic turbulence, *Proc. Roy. Soc. London A* **164**, 192-215.

Kolmogorov A N 1941, Dissipation of energy in the locally isotropic turbulence *Dokl. Akad. Nauk. SSSR* **32**, 15-17., English translation in Proc. R. Soc. Lond. A**434** (1991) 15-17.

Rogers M M and Moser R D 1994 Direct simulatiuon of a self-similar turbulent mixing layer, *Phys. Fluids* **6**, 903-923.

Pearson B and Antonia R A 2001, Reynolds-number dependance of turbulent velocity and pressure increments, *J. Fluid Mech.* **444**, 343-382.

Wygnanski I and Fiedler H E 1968 Some measurements in the self-preserving jet *J. Fluid Mech.* **38**, 527-612.

Yaglom A M 1949 On the local structure of a temperature field in a turbulent flow, *Dokl. Akad. Nauk. SSSR* **69**, 743-746.

Zhou T and Antonia R A 2000 Reynolds number dependance of the small-scale structure of grid turbulence, *J. Fluid Mech*. **406**, 81-107.